

Iodine Doping of CdTe and CdMgTe for Photovoltaic Applications

O.S. OGEDENGBE,^{1,4} C.H. SWARTZ,¹ P.A.R.D. JAYATHILAKA,¹
J.E. PETERSEN,¹ S. SOHAL,¹ E.G. LEBLANC,¹ M. EDIRISOORIYA,¹
K.N. ZAUNBRECHER,² A. WANG,³ T.M. BARNES,² and T.H. MYERS¹

1.—Materials Science, Engineering, and Commercialization Program, 601 University Drive, Texas State University, San Marcos, TX 78666, USA. 2.—National Renewable Energy Laboratory, 15013 Denver West Parkway MS RSF200, Golden, CO 80401, USA. 3.—EAG Laboratories, 810 Kifer Road, Sunnyvale, CA 94086, USA. 4.—e-mail: oso6@txstate.edu

Iodine-doped CdTe and Cd_{1-x}Mg_xTe layers were grown by molecular beam epitaxy. Secondary ion mass spectrometry characterization was used to measure dopant concentration, while Hall measurement was used for determining carrier concentration. Photoluminescence intensity and time-resolved photoluminescence techniques were used for optical characterization. Maximum *n*-type carrier concentrations of $7.4 \times 10^{18} \text{ cm}^{-3}$ for CdTe and $3 \times 10^{17} \text{ cm}^{-3}$ for Cd_{0.65}Mg_{0.35}Te were achieved. Studies suggest that electrically active doping with iodine is limited with dopant concentration much above these values. Dopant activation of about 80% was observed in most of the CdTe samples. The estimated activation energy is about 6 meV for CdTe and the value for Cd_{0.65}Mg_{0.35}Te is about 58 meV. Iodine-doped samples exhibit long lifetimes with no evidence of photoluminescence degradation with doping as high as $2 \times 10^{18} \text{ cm}^{-3}$, while indium shows substantial non-radiative recombination at carrier concentrations above $5 \times 10^{16} \text{ cm}^{-3}$. Iodine was shown to be thermally stable in CdTe at temperatures up to 600°C. Results suggest iodine may be a preferred *n*-type dopant compared to indium in achieving heavily doped *n*-type CdTe.

Key words: CdTe, Cd_{1-x}Mg_xTe, doping, iodine, MBE, solar cell

INTRODUCTION

CdTe is one of the leading materials used in thin film photovoltaic (PV) devices due to some of its basic properties such as its ability to permit both *n*- and *p*-type doping, its relatively high absorption coefficient for photons in the visible range, and its direct band gap of 1.514 eV at room temperature, which is near the optimal bandgap for solar energy conversion. Despite the near optimal bandgap, the highest power conversion efficiency in a CdTe solar cell to date, achieved using polycrystalline CdTe, stands at 21%.¹ This is far less than the Shockley–Queisser limit, which is about 32% for a single-

junction cell under AM 1.5 illumination condition. Research efforts have shown that short circuit current (J_{sc}) is near its theoretical limit, implying that strategies to improve cell efficiency will have to be contingent on improving open-circuit voltage (V_{oc}) and fill factor.² Heavy doping has the potential to improve V_{oc} . There is also evidence that inclusion of a Cd_{1-x}Mg_xTe barrier in a solar cell structure may improve open circuit voltage, and, ultimately, cell efficiency.^{3,4}

Indium (In) is typically the *n*-type dopant of choice and appears to be viable for low doping concentrations. CdTe-based solar cells, however, typically rely on the *n*-side to be heavily doped⁵ at carrier concentrations which have been shown to be problematic for doping with indium.⁶ In addition, indium is not an effective dopant in materials such as CdMgTe which may be useful for heterojunction

formation. The other *n*-type dopants that have been used successfully in CdTe are chlorine (Cl), bromine (Br), and iodine (I). Cl and Br appear to be very similar in terms of maximum donor concentration ($N_D \leq 2 \times 10^{18} \text{ cm}^{-3}$).^{7,8}

I-doping of CdTe grown on (100)-oriented CdZnTe by molecular beam epitaxy (MBE) has been reported to have a doping concentration (N_D) as high as $6.2 \times 10^{18} \text{ cm}^{-3}$ and higher doping efficiency than indium doping of CdTe.⁹ Also, I-doping of CdTe using conventional or metal-organic MBE of CdTe grown on (100)-oriented CdTe and (211)B-oriented GaAs substrates resulted in a N_D as high as $3 \times 10^{18} \text{ cm}^{-3}$. Iodine-doped CdTe samples made with ethyliodide yielded extremely bright excitonic photoluminescence (PL) at 300 K, suggesting that these samples had fewer non-radiative defects.¹⁰ Thus, we have investigated I as an *n*-type dopant for CdTe layers to determine N_D , the photocarrier lifetime τ , and process compatibility in a typical PV device stack.

EXPERIMENT

A DCA Instruments eight-source MBE system was used to grow iodine-doped CdTe and CdMgTe layers. The MBE system maintains a typical base pressure that ranges from 10^{-11} kPa to 10^{-12} kPa, while the operational pressure ranges from 10^{-10} kPa to 10^{-11} kPa. Iodine doping was carried out with the use of ZnI_2 as the solid source since elemental halogens are not compatible with the MBE process due to their high pressures, and ZnI_2 was more readily obtained in a high purity form. A dual-zone low-temperature effusion cell was used for the ZnI_2 source, which is maintained at temperatures lower than 10°C when not in use to limit sublimation and background I. Zn and I incorporate separately,⁷ and the concentration of iodine is double the concentration of Zn in CdTe as verified by SIMS measurement for a wide range of doping flux. The highest atomic density for iodine incorporation in CdTe for this study is low 10^{19} cm^{-3} , making the atomic density of Cd and Te to be greater than iodine or Zn by at least a factor of 10^3 , hence, the effect of Zn on the lattice parameter of CdTe is insignificant. The purity of ZnI_2 source material is 5N, and other source materials have at least 6N purity rating.

CdTe and $\text{Cd}_{0.96}\text{Zn}_{0.04}\text{Te}$ wafers used for this study were purchased from JX Nippon Mining and Metals USA. These wafers, which are 0.8 mm thick and $10 \text{ mm} \times 10 \text{ mm}$ in length and width, were mounted on a 3-inch (c.7.6-cm) substrate holder prior to the MBE growth. InSb wafers used in this study were purchased from Wafer Technology. It was determined that as-received CdTe and CdZnTe substrates had near-surface damage in the top $10 \mu\text{m}$ of the substrate. Surface damage was removed through an etch/polish process. The procedure is carried out by first rinsing the as-received substrates in TCE, acetone and methanol for 10 min

each, followed by a bromine-methanol etch (0.5 vol.%) for 5 min. The substrates then underwent a brief chemi-mechanical polish with a bromine-methanol solution (0.02 vol.%) for 2 min. The polished samples were then rinsed in methanol solution for 2 min, then followed by a 5-min deionized-water rinse and then blown dry with nitrogen.

CdTe films were grown on semi-insulating (100) or (211) CdTe substrates, while $\text{Cd}_{1-x}\text{Mg}_x\text{Te}$ films were grown on semi-insulating (100) $\text{Cd}_{0.96}\text{Zn}_{0.04}\text{Te}$ which provided a closer lattice match. Mg in the CdMgTe films was shielded against oxidation in the air by growing a 10-nm cap layer of CdTe on the CdMgTe layer. Double heterostructures (DH) of CdTe with CdMgTe barriers were also grown on (100) InSb substrates as described elsewhere.¹¹ The heterostructure formed by CdTe and CdMgTe possess a type-I band edge alignment. The wide band gap $\text{Cd}_{1-x}\text{Mg}_x\text{Te}$ barriers, which are made to confine photocarriers and prevent rapid recombination at the CdTe surface, have a thickness of 30 nm and a composition of $x \sim 0.35$, as measured by spectroscopic ellipsometry.¹² The substrate temperature was maintained at 240°C during growth.

After growth, I-doped films of CdTe and CdMgTe were electrically characterized by the Van der Pauw Hall effect technique using a Physical Properties Measurement System manufactured by Quantum Design, with soldered indium as contacts. A few samples were measured as a function of temperature (T) from 20 K to 300 K, and activation energy analysis was carried out.¹³ Iodine incorporation was measured at EAG Laboratories (San Jose, CA, USA) with secondary ion mass spectrometry (SIMS). The detection limit is 1×10^{14} atoms/ cm^3 . Ion implant standards were fabricated to allow accurate quantification of I in CdTe. The CdTe, $\text{Cd}_{0.96}\text{Zn}_{0.04}\text{Te}$, and InSb substrates used in preparing the ion-implanted standards and the substrates used for MBE growth are from the same vendors and are of similar dimension.

In the $\text{Cd}_{1-x}\text{Mg}_x\text{Te}$ films, a linear relationship was established between band gap (E_g) and Mg composition x through cathodoluminescence and energy dispersive x-ray spectroscopy (EDS) measurements on the same sample set, which is estimated as $E_g(x) = 1.606x + 1.503$ with estimated uncertainty in x of ± 0.015 . This relation is used to estimate composition (x) of Mg in CdMgTe layers with band-gap energy of the layer estimated through a variable-angle spectroscopic ellipsometry measurement analysis.¹¹

The DHs were characterized optically. PL measurements relative to excitation power were taken using a $\times 6.5$ objective lens that focused a 514-nm laser light to a $120\text{-}\mu\text{m}$ FWHM Gaussian spot size, which is an approximate measurement of the beam diameter. The resulting PL was collected and focused on a photomultiplier tube while the absolute excitation power was varied with neutral density filters and measured with a calibrated power meter.

The excitation was chosen to be 4.5 MW/m^2 . Time-resolved photoluminescence (TRPL) was measured by time-correlated single photon detection using a 430-nm pulsed laser, which focused on spot size of about $800 \mu\text{m}$ to give an injection level of $7 \times 10^9 \text{ photons/cm}^2$ for a pulse¹⁴ in systems described elsewhere.

Thermal anneals were carried out in quartz ampoules containing the samples and a small piece of Cd which were sealed under vacuum. SIMS measurements were carried out before and after anneal to study distribution of iodine atoms after anneal relative to iodine atoms' position before anneal.

RESULTS

In this study, heavily *n*-type CdTe with carrier concentration up to $7.4 \times 10^{18} \text{ cm}^{-3}$ was easily and reliably achieved with iodine as shown in Fig. 1. Also shown in Fig. 1 are carrier concentrations obtained for $\text{Cd}_{1-x}\text{Mg}_x\text{Te}$ with $x \sim 0.3\text{--}0.35$. I appears to be a good dopant in $\text{Cd}_{1-x}\text{Mg}_x\text{Te}$ with reasonable activation for *n* up to about $3 \times 10^{17} \text{ cm}^{-3}$ at an I concentration of about $\sim 10^{18} \text{ cm}^{-3}$. This result suggest that compensation may be occurring at iodine dopant concentration above $\sim 7 \times 10^{18} \text{ cm}^{-3}$ in CdTe and $\sim 1 \times 10^{18} \text{ cm}^{-3}$ in $\text{Cd}_{0.65}\text{Mg}_{0.35}\text{Te}$.

Based on calibrated SIMS measurements, the typical iodine-doped CdTe sample had an activation of greater than 80%. Consistent with this, temperature-dependent Hall measurements, as shown in Fig. 2, indicated a very low activation energy, less than 10 meV. The room temperature mobility was $800 \text{ cm}^2 \text{ V}^{-1} \text{ s}^{-1}$, consistent with the highest values reported elsewhere for *n*-CdTe.¹⁵ Carrier mobility increased with decreasing temperature as shown in Fig. 3. Also shown is the mobility for $\text{Cd}_{1-x}\text{Mg}_x\text{Te}$ which was observed to decrease with increasing *x* value decreasing by a factor of 2 for $x \sim 0.3$ and then

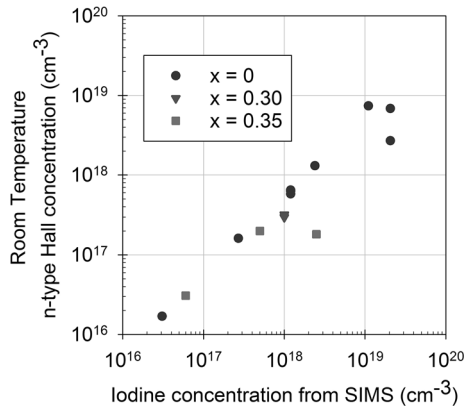


Fig. 1. Electron carrier concentration at 300 K versus calibrated SIMS iodine concentration for iodine-doped CdTe and $\text{Cd}_{1-x}\text{Mg}_x\text{Te}$, illustrating the high level of activation and wide range of electron concentration.

falling precipitously to a room-temperature value of $38 \text{ cm}^2 \text{ V}^{-1} \text{ s}^{-1}$ at $x \sim 0.35$.

The activation energy of iodine in $\text{Cd}_{1-x}\text{Mg}_x\text{Te}$ was determined by fitting the data to the charge balance equation (shown as lines in Fig. 2) and the resulting values are presented in Table I. Activation energy increases with increasing *x* value. The current data suggest a small increase in activation energy with increasing *x* up to $x \sim 0.3$, roughly 2.3 meV for every 0.05 in *x*. Above this value of *x*, the activation energy increased dramatically. The phenomenon underlying the rapid change in electrical properties around $x \sim 0.35$ is not clear and cannot be determined from our limited sample set. Fischer et al. Ref. 16 postulate the presence of a deep donor state for halogen doping, which is pushed into the bandgap with increasing *x*. Their results indicate a rapid decrease in activation occurs for Cl at $x \sim 0.15$ and for Br at $x \sim 0.25\text{--}0.30$. While their data did not indicate a similar feature related to I for their samples with *x* estimated to be comparable to 0.35, there are likely differences between their *x*-determination and ours and it is possible we are at an *x*-value which allows observation of this phenomenon for I.

We note that the $\text{Cd}_{0.65}\text{Mg}_{0.35}\text{Te}$ sample with $n \sim 3 \times 10^{16} \text{ cm}^{-3}$ had an iodine concentration of $6 \times 10^{16} \text{ cm}^{-3}$, which implies that the free carrier concentration of $3 \times 10^{16} \text{ cm}^{-3}$ at room temperature is consistent with the 58 meV activation energy and the decrease is not due to compensation. Little temperature dependence was observed for *n*-type carrier concentration in CdMgTe at doping concentrations above $5 \times 10^{16} \text{ cm}^{-3}$. Similar observation was made in iodine-doped CdTe, where little temperature dependence was observed for doping concentration above $1 \times 10^{17} \text{ cm}^{-3}$.

We have also produced DHs with variable *n*-type iodine doping. The appropriate relationship¹⁴ for

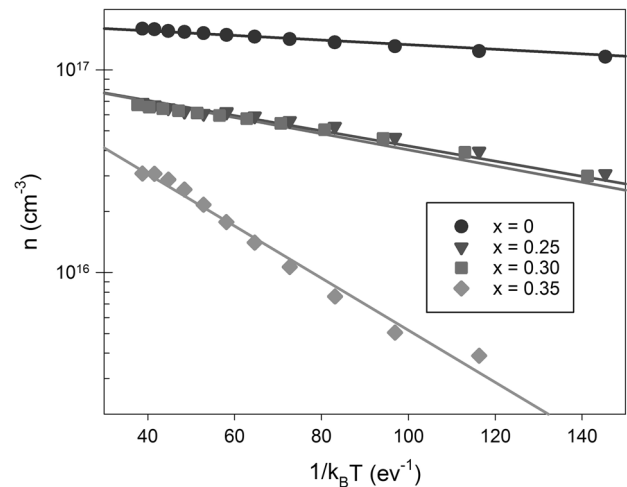


Fig. 2. Temperature dependence of carrier concentration with I concentrations at $\sim 1.1 \pm 0.5 \times 10^{17} \text{ cm}^{-3}$ in CdTe and $\text{Cd}_{1-x}\text{Mg}_x\text{Te}$.

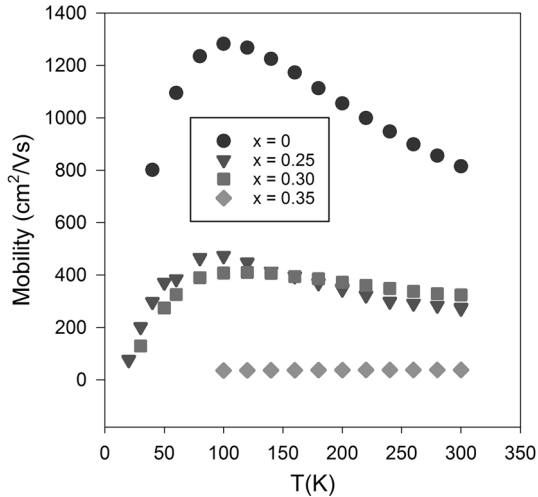


Fig. 3. Temperature dependence of mobility with I concentrations at $\sim 1.1 \pm 0.5 \times 10^{17} \text{ cm}^{-3}$ in CdTe and Cd_{1-x}Mg_xTe.

low-injection TRPL lifetimes in the case of doping is as follows:

$$\frac{1}{\tau_{\text{eff}}} = \frac{1}{\tau_{\text{rad}}} + \frac{1}{\tau_{\text{SRH}}} + \frac{2S}{d} \quad (1)$$

where S is the surface recombination velocity (SRV) and d is absorber thickness. The lifetime due to capture by recombination centers is given as τ_{SRH} . The radiative lifetime is given by

$$\tau_{\text{rad}} = \frac{1}{B_{\text{rad}} n \phi} \quad (2)$$

where n is the carrier concentration and B_{rad} is the radiative parameter. Previous studies analyzing the PL dependence on excitation intensity coupled with TRPL on undoped DHs strongly support a value of $B_{\text{rad}} = 1 \times 10^{-10} \text{ cm}^3 \text{ s}^{-1}$, which is consistent with the Van Roosbroeck–Shockley relationship between absorption and recombination¹⁷ which yields a similar value obtained solely from literature values of the absorption spectrum of CdTe.¹⁸ The parameter ϕ is the photon recycling factor, which recognizes that, in high-quality material, especially in a thick DH configuration, photons emitted in the radiative recombination process can be reabsorbed to create another electron–hole pair, effectively recycling the original pair.¹⁹ It is equal to the probability that a given radiative recombination event’s photon is not absorbed to form a new pair.

Figure 4 contains a plot of the TRPL lifetimes measured for three iodine doping concentrations at various absorber thicknesses in CdTe/Cd_{0.65}Mg_{0.35}Te DHs. Based on prior work carried out by this group, a similar CdMgTe barrier composition resulted in a SRV of 160 cm s^{-1} with nominally undoped absorber material.²⁰ The gray line in the graph illustrates the expected upper limit on TRPL lifetime expected due to surface

Table I. Activation energies of iodine in Cd_{1-x}Mg_xTe at different Mg composition

Mg composition x in Cd _{1-x} Mg _x Te	E_a (meV)
0	6
0.25	17
0.30	20
0.35	58

recombination based on this value. From the results for TRPL shown, it is clear that several values exceed this limit, suggesting that SRV in these doped samples is actually less than 160 cm s^{-1} and on the order 25 cm s^{-1} or less. The radiative lifetimes are also indicated for a given doping concentration, assuming photon recycling is not present ($\phi \sim 1$) and $B_{\text{rad}} = 1 \times 10^{-10} \text{ cm}^3 \text{ s}^{-1}$, are shown along with the TRPL measured for the associated doping concentration. The $n \sim 1 \times 10^{16} \text{ cm}^{-3}$ DHs seem to be reasonably explained without invoking photon recycling. In contrast, the majority of the TRPL lifetimes measured for the $n \sim 1 \times 10^{17} \text{ cm}^{-3}$ and $1 \times 10^{18} \text{ cm}^{-3}$ DHs exceed the radiative limit by factors of 3–6, suggesting that recycling is a significant factor. This effect is consistent with what is observed for doped GaAs/AlGaAs DHs, underscoring that, once surface recombination is controlled, the electronic properties of CdTe are comparable to those of GaAs, with the potential benefits of a slightly lower radiative recombination parameter. In addition to the long lifetimes shown in these iodine-doped samples, there is no evidence of PL degradation with doping as high as $2 \times 10^{18} \text{ cm}^{-3}$ (the highest in a DH grown to date) as shown in Fig. 5.

High-temperature processing under cadmium ambient is needed for activation of As and P, which are being considered for the p -type side of a CdTe-based solar cell.²¹ Therefore, iodine-doped CdTe was annealed at 500°C for 12 h and at 600°C for 24 h in sealed ampoules under Cd overpressure to evaluate the process compatibility of iodine as a dopant in MBE-grown CdTe. The results of these thermal anneals, as shown in Fig. 6, indicate that there is little change in the concentration–depth profile of the annealed samples when compared to that of the as-grown samples, which are pieces from the same epilayer. The profile obtained at 500°C was indistinguishable from the as-grown within measurement error, while there was a small amount of observable diffusion for the 600°C , 24 h anneal. This result suggests that iodine is not a fast-diffusing dopant in epitaxial CdTe. The thermal stability result reported here by our group is consistent with the result obtained in iodine-doped HgCdTe grown by MOCVD²² and by MOVPE.^{23,24}

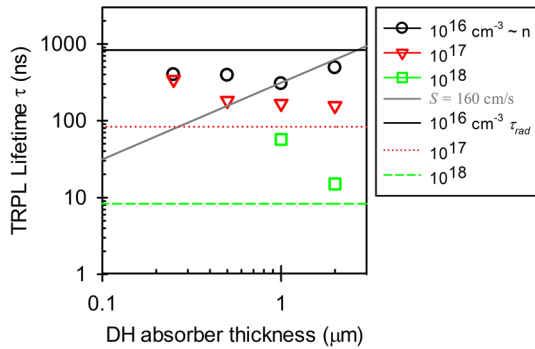


Fig. 4. TRPL lifetimes measured for three doping concentrations at various absorber thicknesses in CdTe/Cd_{0.65}Mg_{0.35}Te DHs. Radiative lifetimes are shown assuming photon recycling is not present ($\varphi \sim 1$) and $B_{rad} = 1 \times 10^{-10} \text{ cm}^3 \text{ s}^{-1}$.

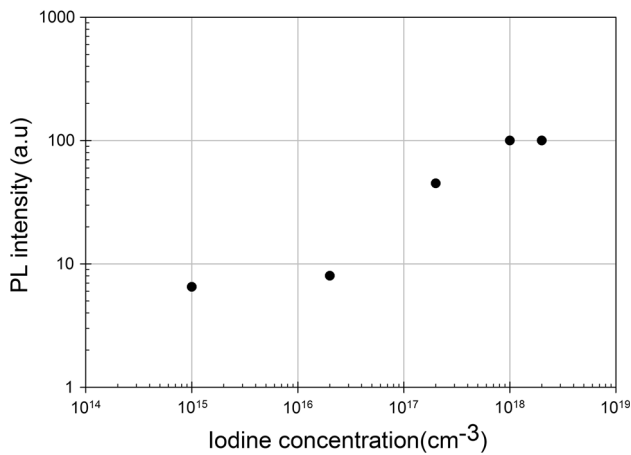


Fig. 5. PL intensity versus iodine concentration in iodine-doped CdTe/CdMgTe DHs at various doping concentrations.

Further investigation was carried out to test the thermal stability behavior of iodine in a p - n epitaxial structure by using a sample that consisted of iodine-doped CdTe steps in a uniformly As-doped CdTe layer. The sample was annealed at 600°C for 24 h under Cd overpressure. SIMS profiles from as-grown and annealed samples, which are pieces from the same epilayer, are shown in Fig. 7. These also suggest that redistribution of iodine atoms after this anneal is small. Several features are noticeable in the profiles shown in Fig. 7. First, as in the layer without As, I diffusion is small for the 600°C, 24-h anneal, suggesting doping levels of As do not affect the I diffusion. Second, the As does not segregate due to the presence of I. Finally, surface accumulation of iodine atoms during the growth of iodine-doped CdTe was noticed in some sample profiles. This surface accumulation was accentuated during As co-doping, as shown by the non-step-like I profiles, yet iodine remains stable to diffusion at anneal temperatures up to 600°C. Modeling the slight differences between as-grown and the 600°C, 24-h annealed samples for both sets indicates an I

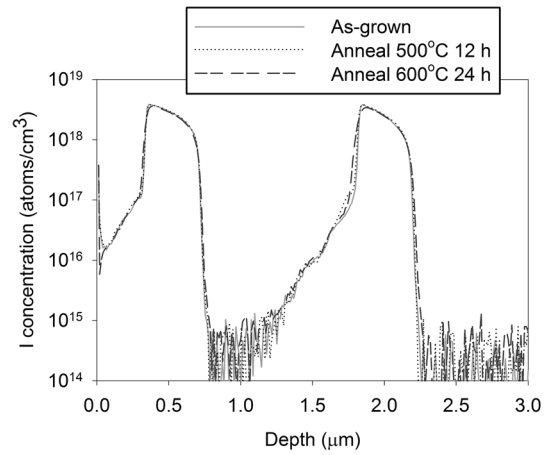


Fig. 6. SIMS profile of an as-grown and an annealed iodine step-doped CdTe sample.

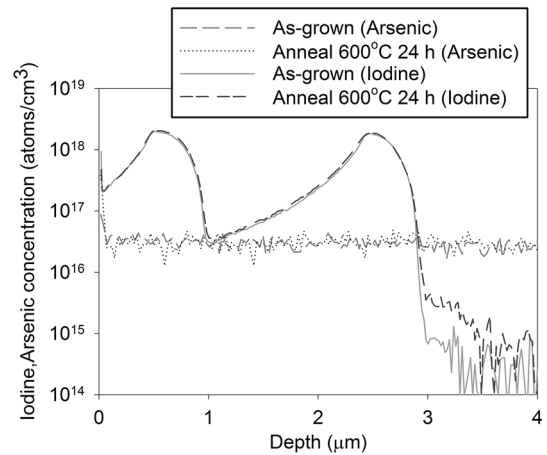


Fig. 7. SIMS profile of an as-grown and an annealed iodine step-doped CdTe:As sample.

diffusion coefficient of $3\text{--}7 \times 10^{-15} \text{ cm}^2 \text{ s}^{-1}$ at 600°C.

CONCLUSIONS

Heavy doping of CdTe can be achieved with iodine without degrading important properties for photovoltaic applications. The n -type doping of CdTe can be accomplished with iodine up to nearly 10^{19} cm^{-3} . It might be possible to achieve a slightly higher maximum doping concentration, but the effect of doping concentration limiting mechanisms become apparent at concentrations above $2 \times 10^{19} \text{ cm}^{-3}$. Doped DHs have a lifetime well in excess of the radiative lifetime due to the photon recycling effect. This is consistent with what is observed for doped GaAs/AlGaAs DHs, underscoring that, once surface recombination is controlled, the electronic properties of CdTe are comparable to those of GaAs, with the potential benefits of a slightly lower radiative recombination parameter and a higher tolerance to dislocations.

These iodine-doped samples show long lifetimes with evidence of photon recycling effects and no evidence of PL degradation, in contrast to indium-doped material, which exhibits significant non-radiative recombination at a carrier concentration above $5 \times 10^{16} \text{ cm}^{-3}$.⁶ Thermal anneal studies of some of these samples suggest that iodine is stable against redistribution at temperatures up to 600°C under Cd overpressure condition. Iodine will not likely diffuse across p - n junction in devices, unlike indium which has been reported to do so more quickly.²⁵ This result, coupled with the longer lifetimes observed for I-doping compared to equivalent In-doping concentration, suggest that iodine may be the preferred dopant when compared with indium.

CdMgTe alloy has been doped with similar success, exhibiting a donor activation energy (E_a) ranging from 17 meV for $x \sim 0.25$ to about 58 meV for $x \sim 0.35$. Iodine has been shown to have significant advantages as a dopant of choice for highly n -type doped CdTe.

ACKNOWLEDGEMENTS

Funding from the Alliance for Sustainable Energy, LLC, the manager and operator of the National Renewable Energy Laboratory for the US Department of Energy. Contract No. DEAC36-08GO28308 FPACE II: Approaching the S-Q Limit with Epitaxial CdTe, Subcontract No. ZEJ-4-42007-0.

REFERENCES

- M.A. Green, K. Emery, Y. Hishikawa, W. Warta, and E.D. Dunlop, *Prog. Photovolt.* 24, 1 (2016).
- H. Zhao, A. Farah, D. Morel, and C. Ferekides, *Thin Solid Films* 517, 2365 (2009).
- Y. Zhao, M. Boccard, S. Liu, J. Becker, X.-H. Zhao, C.M. Campbell, E. Suarez, M.B. Lassise, Z. Holman, and Y.-H. Zhang, *Nat. Energy* 1, 16067 (2016).
- J.J. Becker, C.M. Campbell, Y. Zhao, M. Boccard, D. Mohanty, E. Suarez, M. Lassise, I. Bhat, Y.-H. Zhang, in *Proceedings of the 2016 IEEE 43rd Photovoltaic Specialists Conference* (2016), p. 1421.
- R. Scheer and H.W. Schock, *Chalcogenide Photovoltaics: Physics, Technologies, and Thin Film Devices* (Weinheim: Wiley, 2011), pp. 137–145.
- X.-H. Zhao, S. Liu, Y. Zhao, C.M. Campbell, M.B. Lassise, Y.-S. Kuo, and Y.-H. Zhang, *IEEE J. Photovolt.* 6, 552 (2016).
- A. Waag, T. Litz, F. Fischer, H. Heinke, S. Scholl, D. Hommel, G. Landwehr, and G. Bilger, *J. Cryst. Growth* 138, 437 (1994).
- F. Bassani, S. Tatarenko, K. Kheng, P. Jouneau, K. Saminadayar, N. Magnea, and R. Cox, *Appl. Phys. Lett.* 63, 2106 (1993).
- D. Brun-Le-Cunff, T. Baron, B. Daudin, S. Tatarenko, and B. Blanchard, *Appl. Phys. Lett.* 67, 965 (1995).
- N.C. Giles, J. Lee, T.H. Myers, Z. Yu, B.K. Wagner, R.G. Benz, and C.J. Summers, *J. Electron. Mater.* 24, 691 (1995).
- C.H. Swartz, K.N. Zaunbrecher, S. Sohal, E.G. LeBlanc, M. Edirisooriya, O.S. Ogedengbe, J.E. Petersen, P.A.R.D. Jayathilaka, T.H. Myers, M.W. Holtz, and T.M. Barnes, *J. Appl. Phys.* 120, 165305 (2016).
- C.H. Swartz, M. Edirisooriya, E.G. LeBlanc, O.C. Noriega, P.A.R.D. Jayathilaka, O.S. Ogedengbe, B.L. Hancock, M. Holtz, T.H. Myers, and K.N. Zaunbrecher, *Appl. Phys. Lett.* 105, 222107 (2014).
- D.C. Look, *Electrical Characterization of GaAs Materials and Devices* (New York: Wiley, 1989), p. 115.
- S. Sohal, M. Edirisooriya, O. Ogedengbe, J. Petersen, C. Swartz, E. LeBlanc, T. Myers, J. Li, and M. Holtz, *J. Phys. D Appl. Phys.* 49, 505104 (2016).
- R.N. Bicknell, N.C. Giles, and J.F. Schetzina, *Appl. Phys. Lett.* 49, 1095 (1986).
- F. Fischer, A. Waag, G. Bilger, T. Litz, S. Scholl, M. Schmitt, and G. Landwehr, *J. Cryst. Growth* 141, 93 (1994).
- W. Van Roosbroeck and W. Shockley, *Phys. Rev.* 94, 1558 (1954).
- A. Rakhshani, *J. Appl. Phys.* 81, 7988 (1997).
- X.-H. Zhao, M.J. DiNezza, S. Liu, C.M. Campbell, Y. Zhao, and Y.-H. Zhang, *Appl. Phys. Lett.* 105, 252101 (2014).
- K.N. Zaunbrecher, D. Kuciauskas, C.H. Swartz, P. Dippo, M. Edirisooriya, O.S. Ogedengbe, S. Sohal, B.L. Hancock, E.G. LeBlanc, and P.A. Jayathilaka, *Appl. Phys. Lett.* 109, 091904 (2016).
- J.M. Burst, J.N. Duenow, D.S. Albin, E. Colegrove, M.O. Reese, J.A. Aguiar, C.-S. Jiang, M. Patel, M.M. Al-Jassim, and D. Kuciauskas, *Nat. Energy* 1, 16015 (2016).
- S. Murakami, T. Okamoto, K. Maruyama, and H. Takigawa, *Appl. Phys. Lett.* 63, 899 (1993).
- C. Maxey, C. Jones, N. Metcalfe, R. Catchpole, M. Houlton, A. White, N. Gordon, and C. Elliott, *J. Electron. Mater.* 25, 1276 (1996).
- C. Maxey, J. Camplin, I. Guilfooy, J. Gardner, R. Lockett, C. Jones, P. Capper, M. Houlton, and N. Gordon, *J. Electron. Mater.* 32, 656 (2003).
- S. Kasap and P. Capper, *Springer Handbook of Electronic and Photonic Materials* (New York: Springer, 2007), p. 316.